Первое наблюдение радиальных возбуждений Bc-мезона

А.Лиходед ОТФ

Предложение по поиску

Prospects for the B_c Studies at LHCb

I.P.Gouz, V.V.Kiselev, A.K.Likhoded, V.I.Romanovsky,
and O.P.Yushchenko

IHEP, Protvino, Russia

Abstract

We discuss the motivations and perspectives for the studies of the mesons of the (bc) family at LHCb. The description of production and decays at LHC energies is given in details. The event yields, detection efficiencies, and background conditions for several B_c decay modes at LHCb are estimated.

Спектр масс Bc

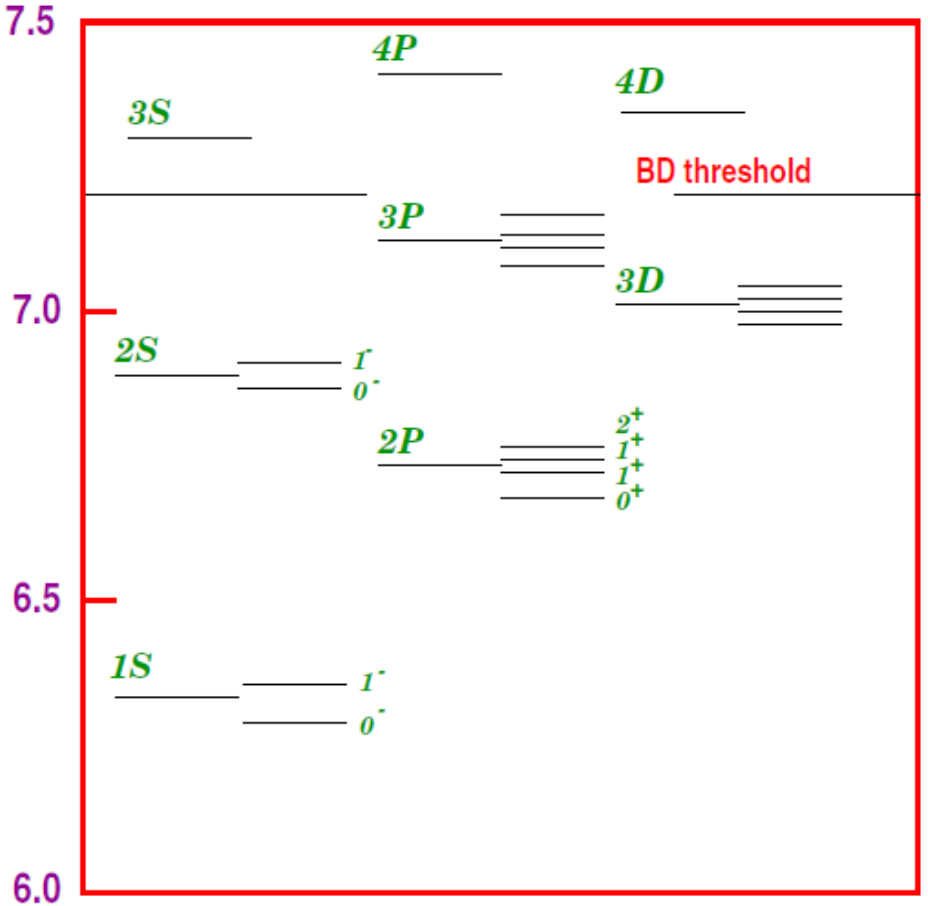

state	Martin	BT
1^1S_0	6.253	6.264
1^1S_1	6.317	6.337
2^1S_0	6.867	6.856
2^1S_1	6.902	6.899
2^1P_0	6.683	6.700
$2P\ 1^+$	6.717	6.730
$2P\ 1'^+$	6.729	6.736
2^3P_2	6.743	6.747
3^1P_0	7.088	7.108
$3P\ 1^+$	7.113	7.135
$3P\ 1'^+$	7.124	7.142
3^3P_2	7.134	7.153
$3D\ 2^-$	7.001	7.009
3^5D_3	7.007	7.005
3^3D_1	7.008	7.012
$3D\ 2'^-$	7.016	7.012

Figure 1: The mass spectrum of $(\bar{b}c)$ with account for the spin-dependent splittings.

Переходы Bc

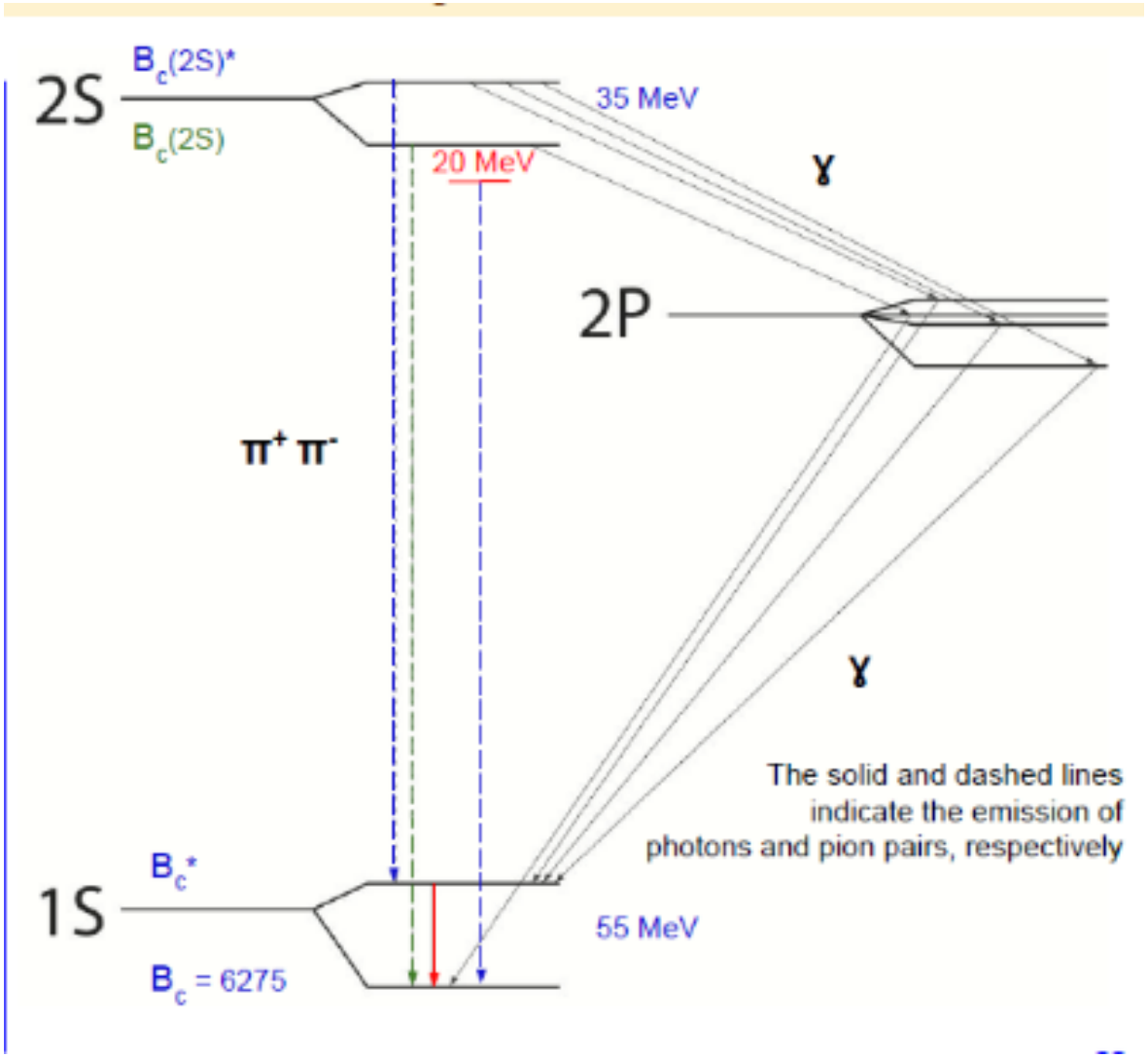
2S
$B_c(2S)^*$
$B_c(2S)$
35 MeV
20 MeV
γ
2P
$\pi^+ \pi^-$
γ
The solid and dashed lines
indicate the emission of
photons and pion pairs, respectively
1S
B_c^*
B_c = 6275
55 MeV

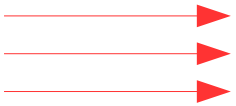

state	Γ_{tot}, KeV	dominant decay mode	BR, %
1^1S_1	0.06	$1^1S_0+\gamma$	100
2^1S_0	67.8	$1^1S_0+\pi\pi$	74
2^1S_1	86.3	$1^1S_1+\pi\pi$	58
2^1P_0	65.3	$1^1S_1+\gamma$	100
$2P\ 1^+$	89.4	$1^1S_1+\gamma$	87
$2P\ 1'^+$	139.2	$1^1S_0+\gamma$	94
2^3P_2	102.9	$1^1S_1+\gamma$	100
3^1P_0	44.8	$2^1S_1+\gamma$	57
$3P\ 1^+$	65.3	$2^1S_1+\gamma$	49
$3P\ 1'^+$	92.8	$2^1S_0+\gamma$	63
3^3P_2	71.6	$2^1S_1+\gamma$	69
$3D\ 2^-$	95.0	$2P\ 1^+ + \gamma$	47
3^5D_3	107.9	$2^3P_2+\gamma$	71
3^3D_1	155.4	$2^1P_0+\gamma$	51
$3D\ 2'^-$	122.0	$2P\ 1'^+ + \gamma$	38

Table 1: The total widths of $(\bar{b}c)$-states with Martin potential

Mode	Γ [16]	Γ [15]	Γ [17]	Γ [18]	Γ [19]	Γ [20]
$B_c^+ \to \eta_c e^+ \nu$	11	11.1	14.2	14	10.4	8.6
$B_c^+ \to \eta_c \tau^+ \nu$	3.3			3.8		2.9
$B_c^+ \to \eta_c' e^+ \nu$	0.60		0.73		0.74	
$B_c^+ \to \eta_c' \tau^+ \nu$	0.050					
$B_c^+ \to J/\psi e^+ \nu$	28	30.2	34.4	33	16.5	18
$B_c^+ \to J/\psi \tau^+ \nu$	7.0			8.4		5.0
$B_c^+ \to \psi' e^+ \nu$	1.94		1.45		3.1	
$B_c^+ \to \psi' \tau^+ \nu$	0.17					
$B_c^+ \to D^0 e^+ \nu$	0.059	0.049	0.094	0.26	0.026	
$B_c^+ \to D^0 \tau^+ \nu$	0.032			0.14		
$B_c^+ \to D^{*0} e^+ \nu$	0.27	0.192	0.269	0.49	0.053	
$B_c^+ \to D^{*0} \tau^+ \nu$	0.12			0.27		
$B_c^+ \to B_s^0 e^+ \nu$	59	14.3	26.6	29	13.8	15
$B_c^+ \to B_s^{*0} e^+ \nu$	65	50.4	44.0	37	16.9	34
$B_c^+ \to B^0 e^+ \nu$	4.9	1.14	2.30	2.1		
$B_c^+ \to B^{*0} e^+ \nu$	8.5	3.53	3.32	2.3		

Table 3: Exclusive widths of semileptonic B_c^+ decays, Γ in 10^{-15} GeV.

Table 5: Branching ratios [16] of exclusive B_c^+ decays at the fixed choice of factors: $a_1^c = 1.20$ and $a_2^c = -0.317$ in the non-leptonic decays of c quark, and $a_1^b = 1.14$ and $a_2^b = -0.20$ in the non-leptonic decays of $\bar{b}$ quark. The lifetime of B_c is appropriately normalized by $\tau[B_c] \approx 0.45$ ps.

Mode	BR, %	Mode	BR, %	Mode	BR, %
$B_c^+ \to \eta_c e^+ \nu$	0.75	$B_c^+ \to J/\psi K^+$	0.011	$B_c^+ \to B_s^0 K^+$	1.06
$B_c^+ \to \eta_c \tau^+ \nu$	0.23	$B_c \to J/\psi K^{*+}$	0.022	$B_c^+ \to B_s^{*0} K^+$	0.37
$B_c^+ \to \eta_c' e^+ \nu$	0.041	$B_c^+ \to D^+ \overline{D}^0$	0.0053	$B_c^+ \to B_s^0 K^{*+}$	–
$B_c^+ \to \eta_c' \tau^+ \nu$	0.0034	$B_c^+ \to D^+ \overline{D}^{*0}$	0.0075	$B_c^+ \to B_s^{*0} K^{*+}$	–
$B_c^+ \to J/\psi e^+ \nu$	1.9	$B_c^+ \to D^{*+} \overline{D}^0$	0.0049	$B_c^+ \to B^0 \pi^+$	1.06
$B_c^+ \to J/\psi \tau^+ \nu$	0.48	$B_c^+ \to D^{*+} \overline{D}^{*0}$	0.033	$B_c^+ \to B^0 \rho^+$	0.96
$B_c^+ \to \psi' e^+ \nu$	0.132	$B_c^+ \to D_s^+ \overline{D}^0$	0.00048	$B_c^+ \to B^{*0} \pi^+$	0.95
$B_c^+ \to \psi' \tau^+ \nu$	0.011	$B_c^+ \to D_s^+ \overline{D}^{*0}$	0.00071	$B_c^+ \to B^{*0} \rho^+$	2.57
$B_c^+ \to D^0 e^+ \nu$	0.004	$B_c^+ \to D_s^{*+} \overline{D}^0$	0.00045	$B_c^+ \to B^0 K^+$	0.07
$B_c^+ \to D^0 \tau^+ \nu$	0.002	$B_c^+ \to D_s^{*+} \overline{D}^{*0}$	0.0026	$B_c^+ \to B^0 K^{*+}$	0.015
$B_c^+ \to D^{*0} e^+ \nu$	0.018	$B_c^+ \to \eta_c D_s^+$	0.86	$B_c^+ \to B^{*0} K^+$	0.055
$B_c^+ \to D^{*0} \tau^+ \nu$	0.008	$B_c^+ \to \eta_c D_s^{*+}$	0.26	$B_c^+ \to B^{*0} K^{*+}$	0.058
$B_c^+ \to B_s^0 e^+ \nu$	4.03	$B_c^+ \to J/\psi D_s^+$	0.17	$B_c^+ \to B^+ \overline{K^0}$	1.98
$B_c^+ \to B_s^{*0} e^+ \nu$	5.06	$B_c^+ \to J/\psi D_s^{*+}$	1.97	$B_c^+ \to B^+ \overline{K^{*0}}$	0.43
$B_c^+ \to B^0 e^+ \nu$	0.34	$B_c^+ \to \eta_c D^+$	0.032	$B_c^+ \to B^{*+} \overline{K^0}$	1.60
$B_c^+ \to B^{*0} e^+ \nu$	0.58	$B_c^+ \to \eta_c D^{*+}$	0.010	$B_c^+ \to B^{*+} \overline{K^{*0}}$	1.67
$B_c^+ \to \eta_c \pi^+$	0.20	$B_c^+ \to J/\psi D^+$	0.009	$B_c^+ \to B^+ \pi^0$	0.037
$B_c^+ \to \eta_c \rho^+$	0.42	$B_c^+ \to J/\psi D^{*+}$	0.074	$B_c^+ \to B^+ \rho^0$	0.034
$B_c^+ \to J/\psi \pi^+$	0.13	$B_c^+ \to B_s^0 \pi^+$	16.4	$B_c^+ \to B^{*+} \pi^0$	0.033
$B_c^+ \to J/\psi \rho^+$	0.40	$B_c^+ \to B_s^0 \rho^+$	7.2	$B_c^+ \to B^{*+} \rho^0$	0.09
$B_c^+ \to \eta_c K^+$	0.013	$B_c^+ \to B_s^{*0} \pi^+$	6.5	$B_c^+ \to \tau^+ \nu_\tau$	1.6
$B_c^+ \to \eta_c K^{*+}$				$B_c^+ \to c\bar{s}$	4.9

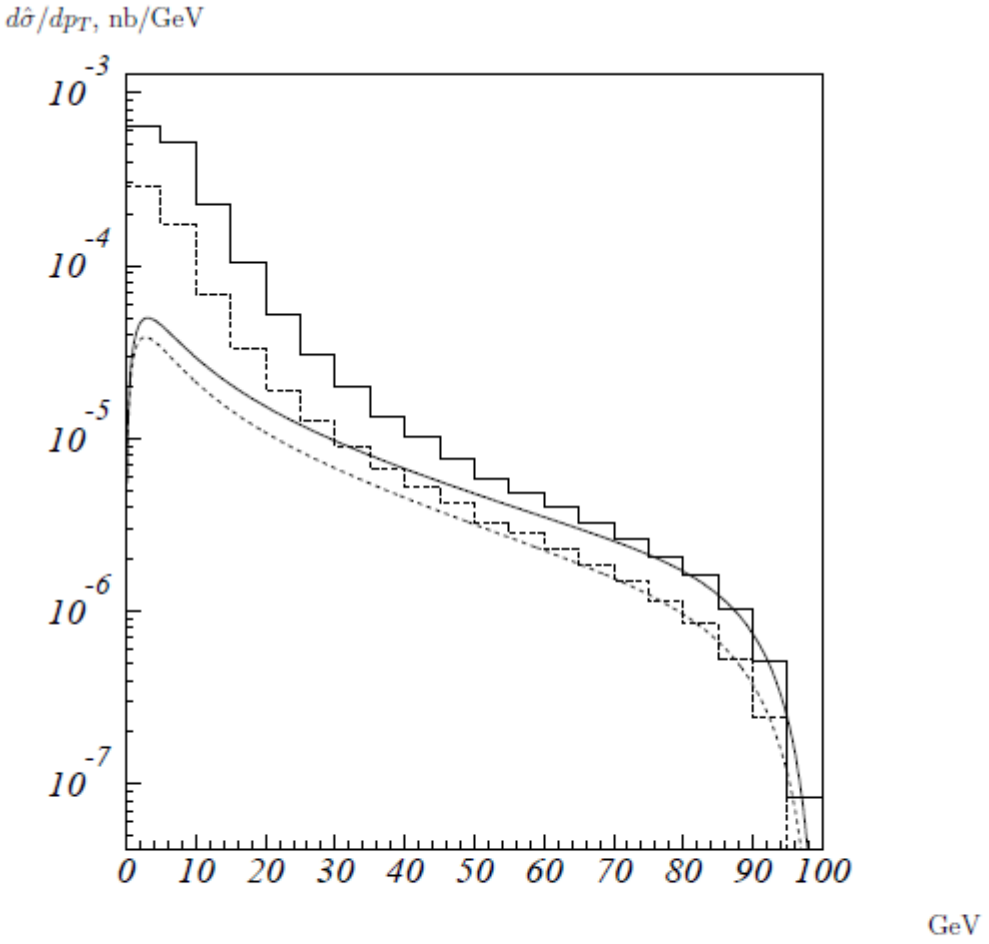

Figure 3: The differential cross-section for the $B_c^{(*)}$ meson production in gluon-gluon collisions as calculated in the perturbative QCD over the complete set of diagrams in the $O(\alpha_s^4)$ order at 200 GeV. The dashed and solid histograms present the pseudoscalar and vector states, respectively, in comparison with the corresponding results of fragmentation model shown by the smooth curves.

Численные результаты для LHC

The using of CTEQ5L parameterization for the structure functions of nucleon [40] leads to the total hadronic cross-sections for the B_c mesons of about 0.8 μb that accepts contributions from:

$1S_0$	$1S_1$	$2S_0$	$2S_1$
0.19 μb	0.47 μb	0.05 μb	0.11 μb

After the summing over the different spin states, the total cross-sections for the production of P-wave levels is equal to 7% of the S-state cross-section.

At LHC with the luminosity $\mathcal{L} = 10^{34}$ cm^{-2}s^{-1} and $\sqrt{s} = 14$ TeV one could expect $4.5 \cdot 10^{10}$ B_c^+ events per year.

Nevertheless, the P-wave states could be of a particular interest due to their radiative decays with relatively energetic photons (around 500 MeV in the B_c rest frame). For P-wave states, the leading color-singlet matrix element and the leading color-octet matrix elements are both suppressed by a factor of v^2 (relative velocity of the charmed quark) relative to the color-singlet matrix element for S-wave that can enhance the P-vawe contribution.

Первое наблюдение!

CMS-BPH-18-007:

Observation of two excited B_c^+ states and measurement of the $B_c^+(2S)$ mass in pp collisions at $\sqrt{s} = 13$ TeV

Submitted to Phys. Rev. Lett. (arXiv:1902.00571)

Introduction

The B_c meson was discovered in 1998 by CDF. **PRL 81 (1998) 2432**
It is the lowest-mass bound state of the family of mesons composed of a charm quark and a bottom anti-quark.

Experimental information is limited by rare production rate, α_s^4 : qqbar, gg → (c-bbar) b-cbar.

Given the different heavy quark flavors, the only allowed transitions are through photons or pion pairs

Particle	Predicted M(MeV)
B_c	6247-6286
B_c^*	6308-6341
$B_c(2S)$	6835-6882
$B_c(2S)^*$	6881-6914

PRD 49 (1994) 5845, PRD 51 (1995) 3613, PRD 52 (1995) 5229, PRD 53 (1996) 312, PLB 382 (1996) 131, PRD 160 (1999) 074006, PRD 67 (2003) 014027, PRD 70 (2004) 054017, PRL 104 (2010) 022001, PRD 86 (2012) 094510, PRL 121 (2018) 202002

PRD 49 (1994) 5845

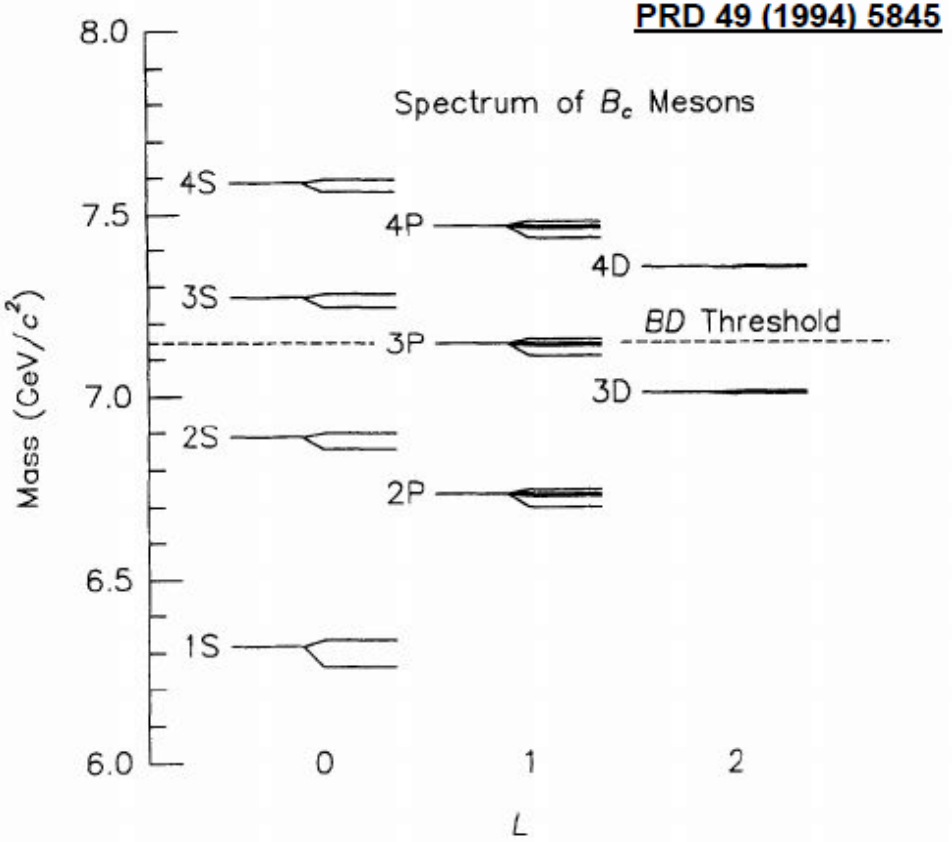

Observation of an excitate B_c meson state by ATLAS

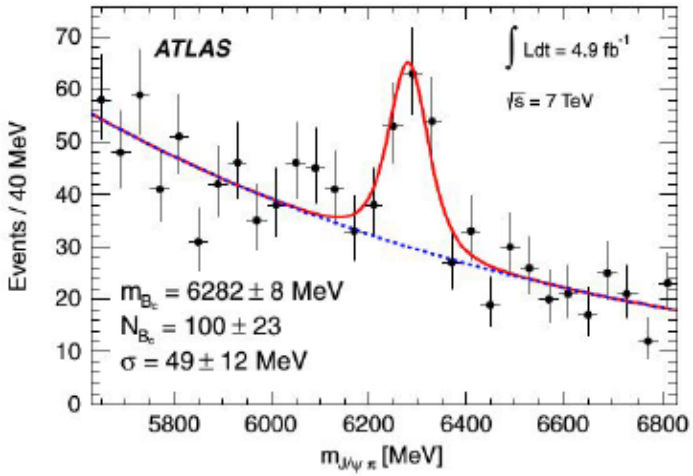

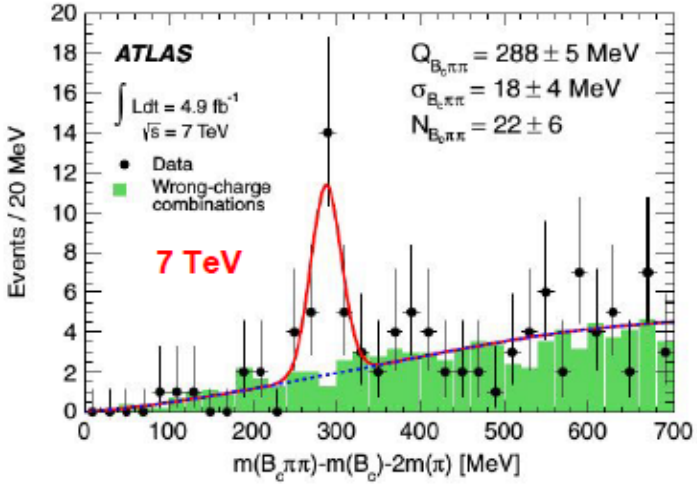

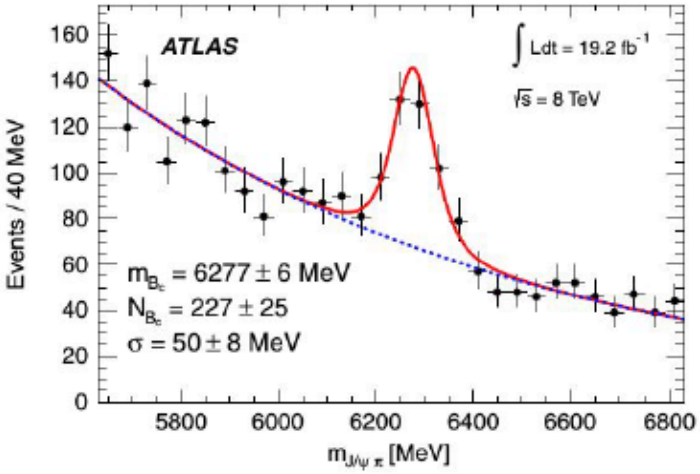

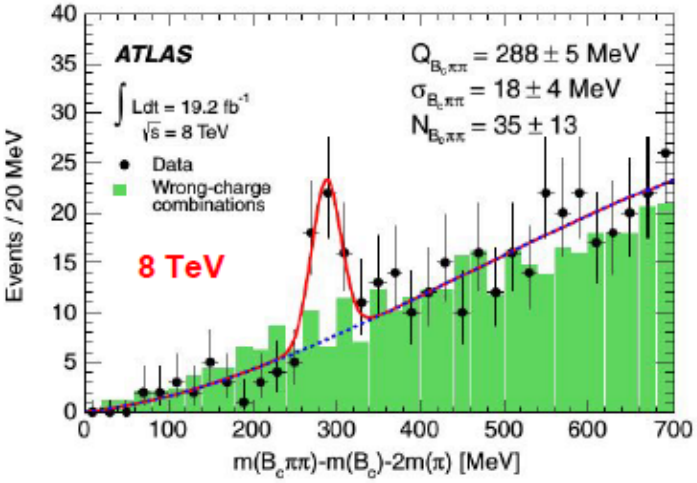

PRL 113, 212004 (2014)

They report the observation of a new state whose mass is consistent with predictions for the $B_c(2S)$

The $B_c(2S)$ is reconstructed from the decay

$B_c \pi^+ \pi^-$ followed by $B_c \rightarrow J/\psi \pi$

with a local significance of 5.4 σ

Reconstruction of the $B_c\pi\pi$

The $B_c(2S)^*$ decays to the B_c ground state through the emission of two pions and a soft photon (around 55 MeV in rest frame) :

$B_c(2S)^* \rightarrow B_c^* \pi^+ \pi^-$ followed by $B_c^* \rightarrow B_c \gamma_{lost}$

Since the photon is not detected, we end up seeing

$B_c(2S)^* \rightarrow B_c \pi^+ \pi^-$ plus "missing energy"

Same final state as

$B_c(2S) \rightarrow B_c \pi^+ \pi^-$

So, we see a two-peak structure in the $B_c \pi^+ \pi^-$ mass distribution, with the $B_c(2S)^*$ peak at a mass shifted by

$$\Delta M = [\, M(B_c^*) - M(B_c) \,] - [\, M(B_c(2S)^*) - M(B_c(2S)) \,]$$

which is predicted to be around 20 MeV.

One have to notice:

$$[\, M(B_c(1S)^*) - M(B_c(1S)) \,] > [\, M(B_c(2S)^*) - M(B_c(2S)) \,]$$

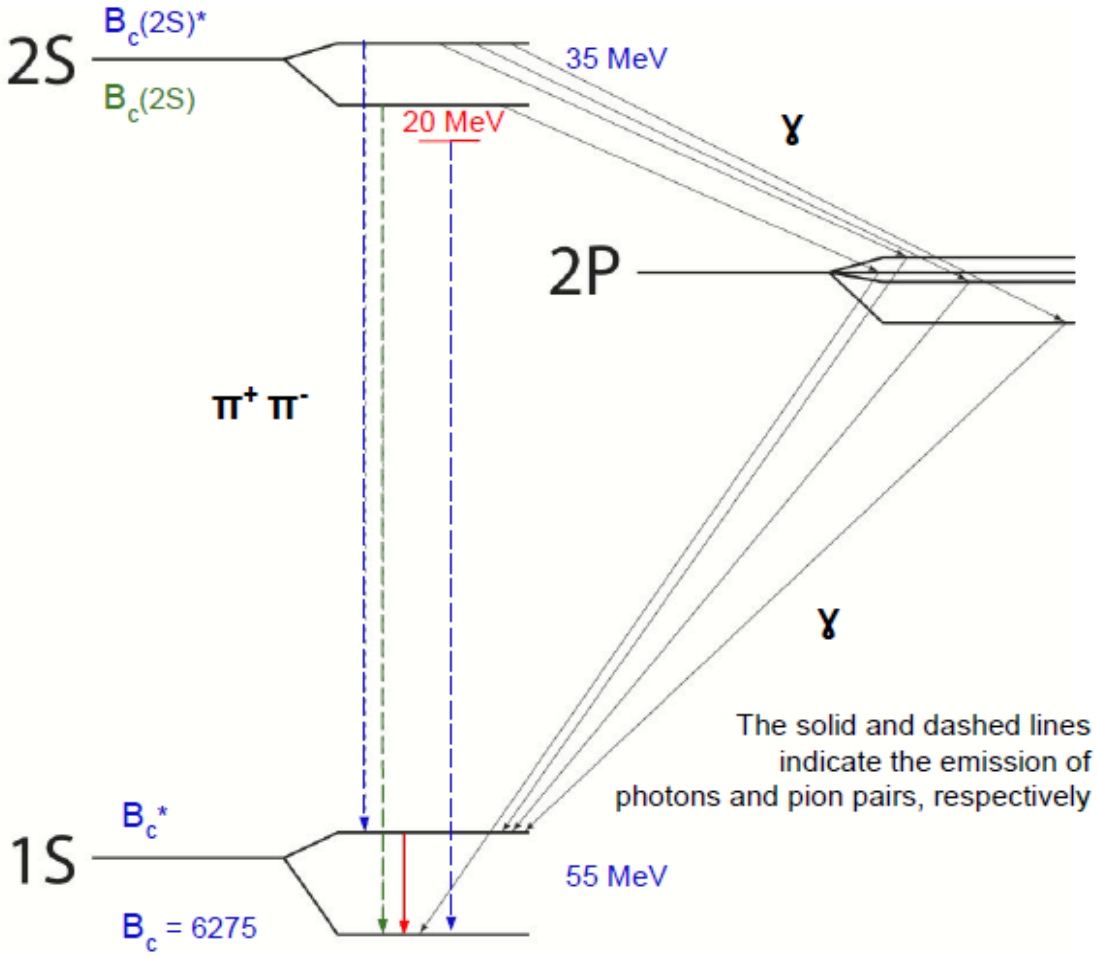

Reconstruction of B_c in data: 2016 + 2017 + 2018

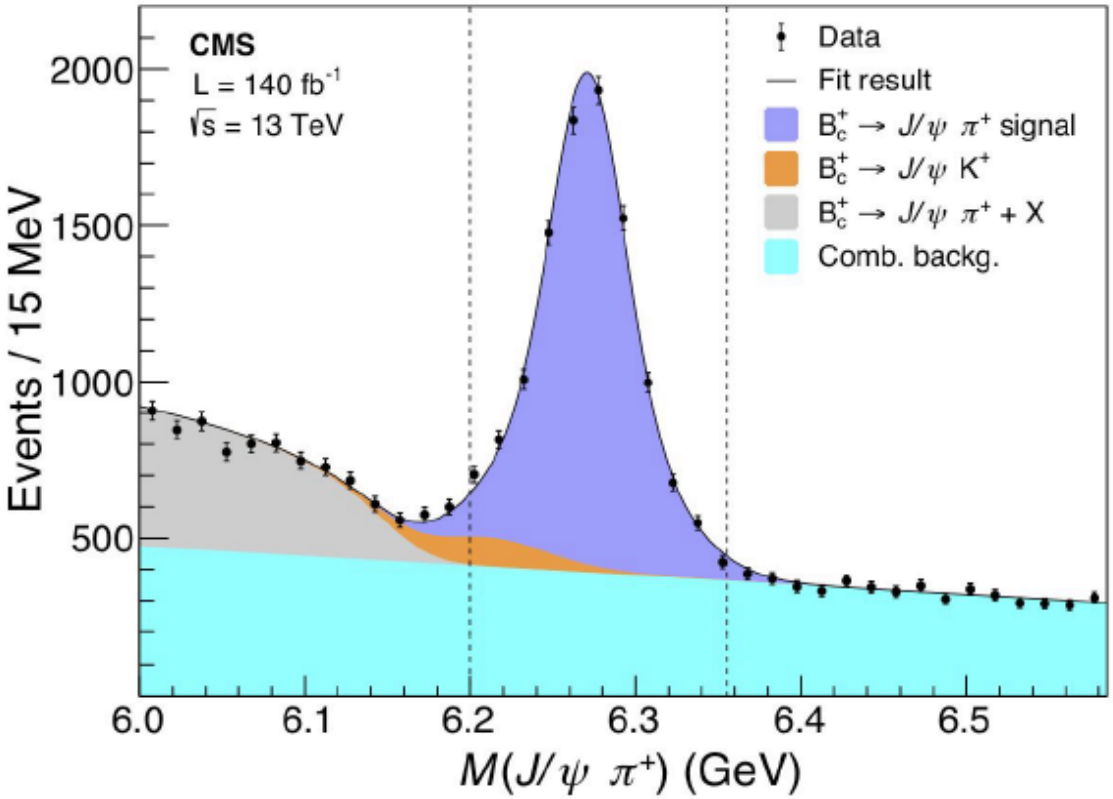

7495 ± 225 candidates

~34 MeV mass resolution

Fit details:

Unbinned ML; the signal is modeled using a double Gaussian with common mean and the background as a polynomial.
Additional background contributions from $B_c \rightarrow J/\psi\ K$ decay is modeled from the simulated sample,
while the partially reconstructed $B_c \rightarrow J/\psi\ \pi\ X$ decays are modeled with an ARGUS function convolved with a Gaussian.

Event selection

kinematic requirements

$p_T(\pi_1) > 3.5$ GeV
B_c prob(vtx) > 0.1
$p_T(B_c) > 15$ GeV
B_c decay length > 0.01 cm
$6.2 < M(B_c) < 6.35$ GeV
$B_c \pi \pi$ prob(vtx) > 0.1
$p_T(\pi_2) > 0.8$, $p_T(\pi_3) > 0.6$ GeV

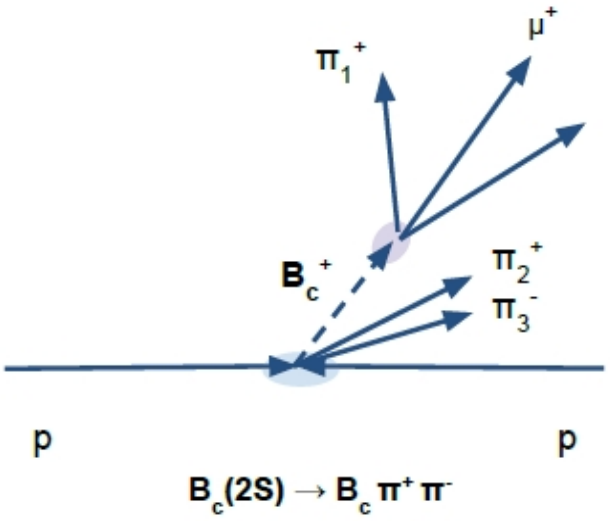

$B_c(2S) \rightarrow B_c \pi^+ \pi^-$

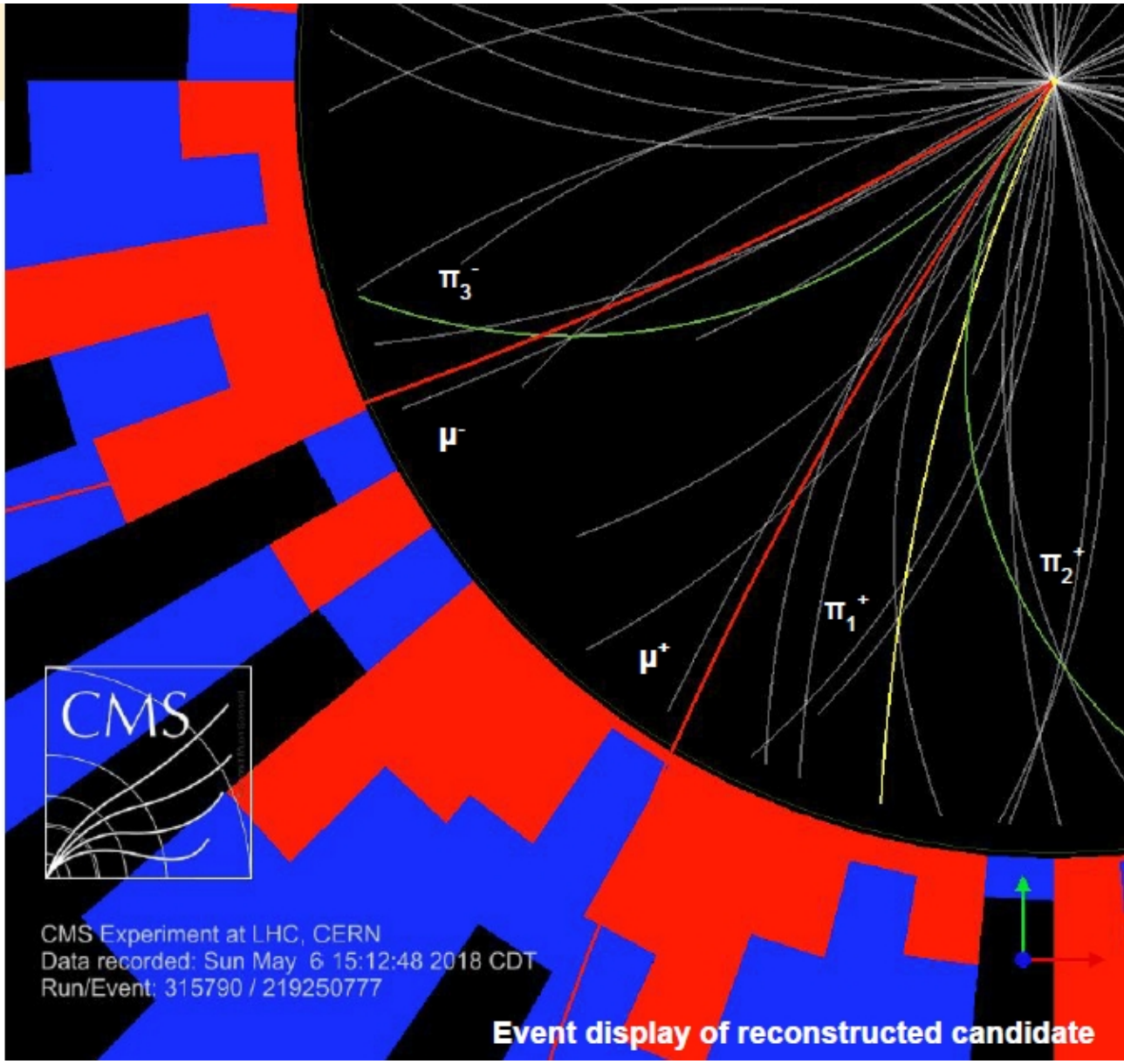

Observation of the two-peak structure

The mass difference between the two states in the $B_c \pi^+\pi^-$ mass distribution is predicted to be $M(B_c(2S)) - \Delta M$, where

$$\Delta M = [\, M(B_c^*) - M(B_c)] - [\, M(B_c(2S)^*) - M(B_c(2S))] \quad \rightarrow \quad \sim 20 \text{ MeV}$$

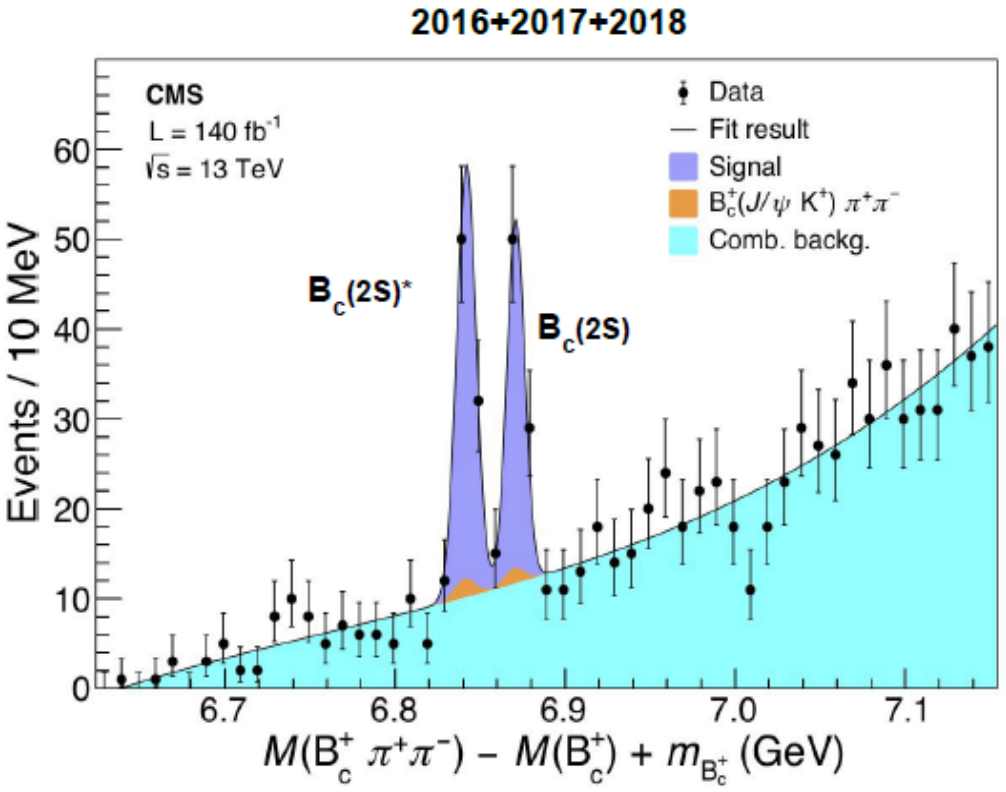

Mass distribution fitted with Gaussian functions for the peaks and a 3rd order polynomial for the background.

Mass resolution agrees with MC expectations ~ 6 MeV

Two-peak structure observed (well resolved) :

$\Delta M = 29.0 \pm 1.5$ (stat) MeV

Local significance exceeding six σ for observing two peaks rather than one, evaluated through the ratio of likelihoods (including syst.). Each of them above five σ

Mass of $B_c(2S)$ measured to be:

$M(B_c(2S)) = 6871.0 \pm 1.2$ (stat) MeV

Natural widths : (50-90 keV predicted)

measurements consistent with zero, e.g. smaller than the resolution

How do we compare with ATLAS observation?

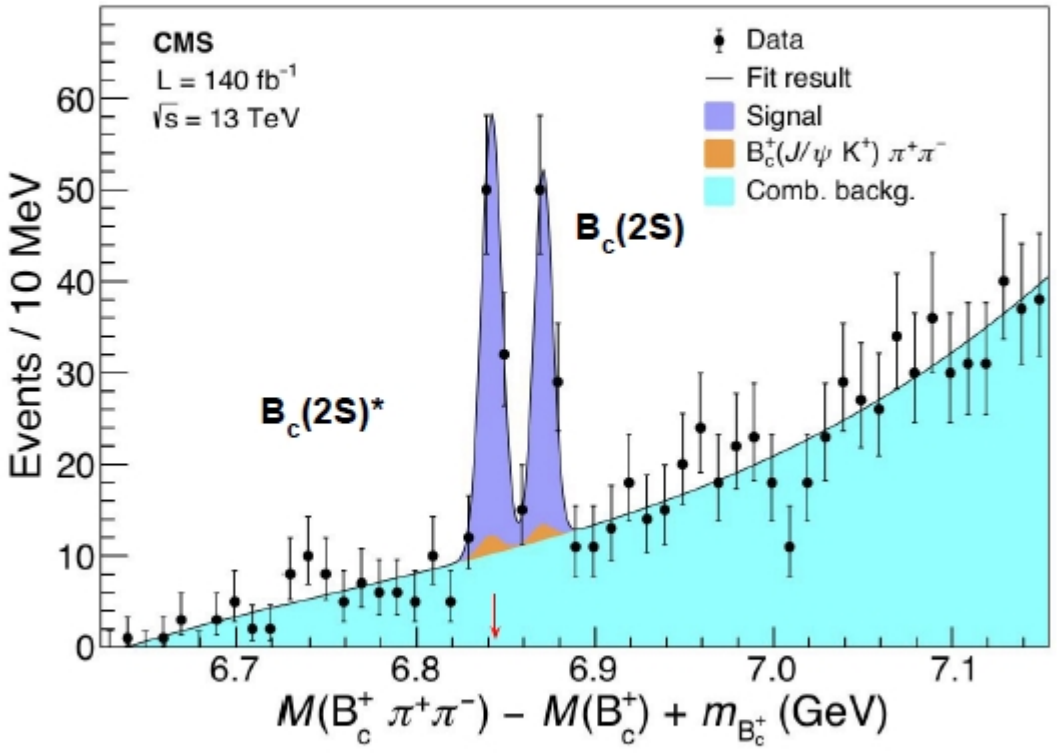

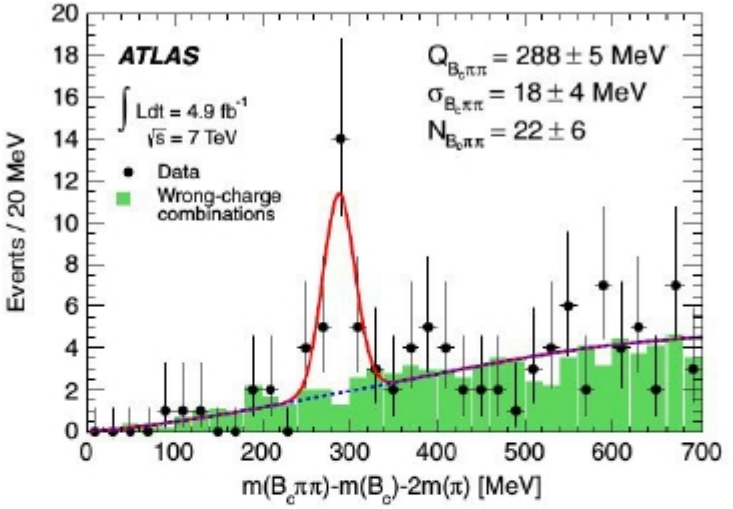

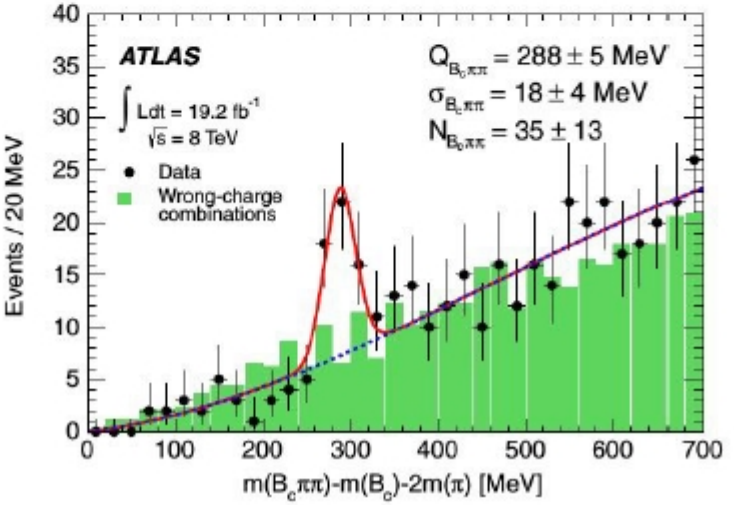

What have we measured in the $B_c\pi\pi$ spectrum?

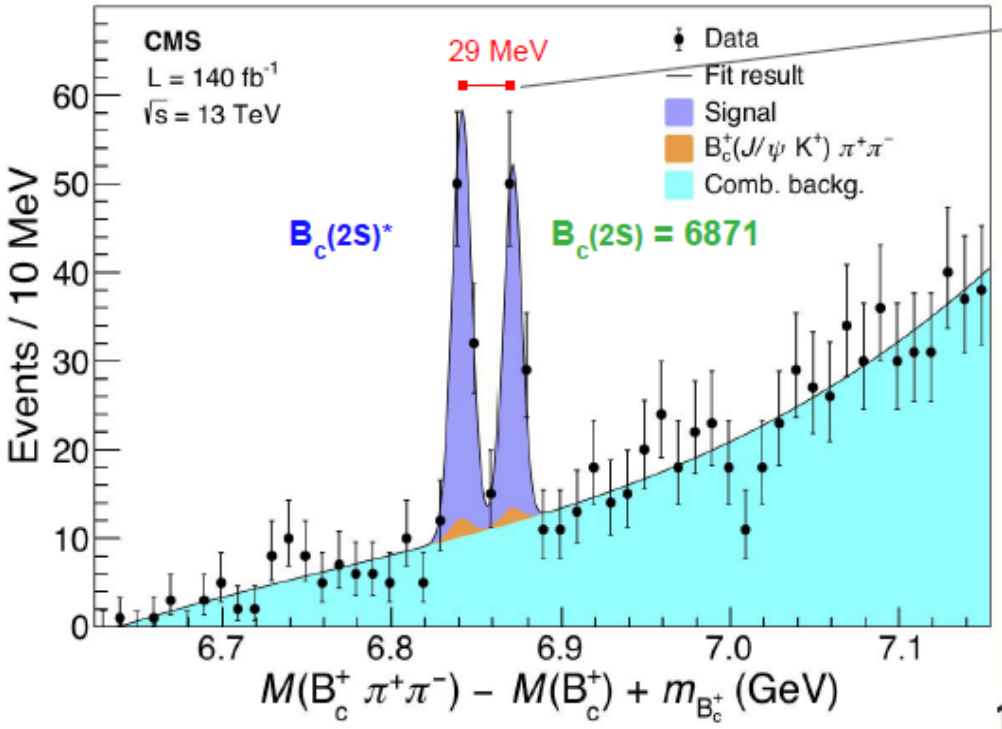

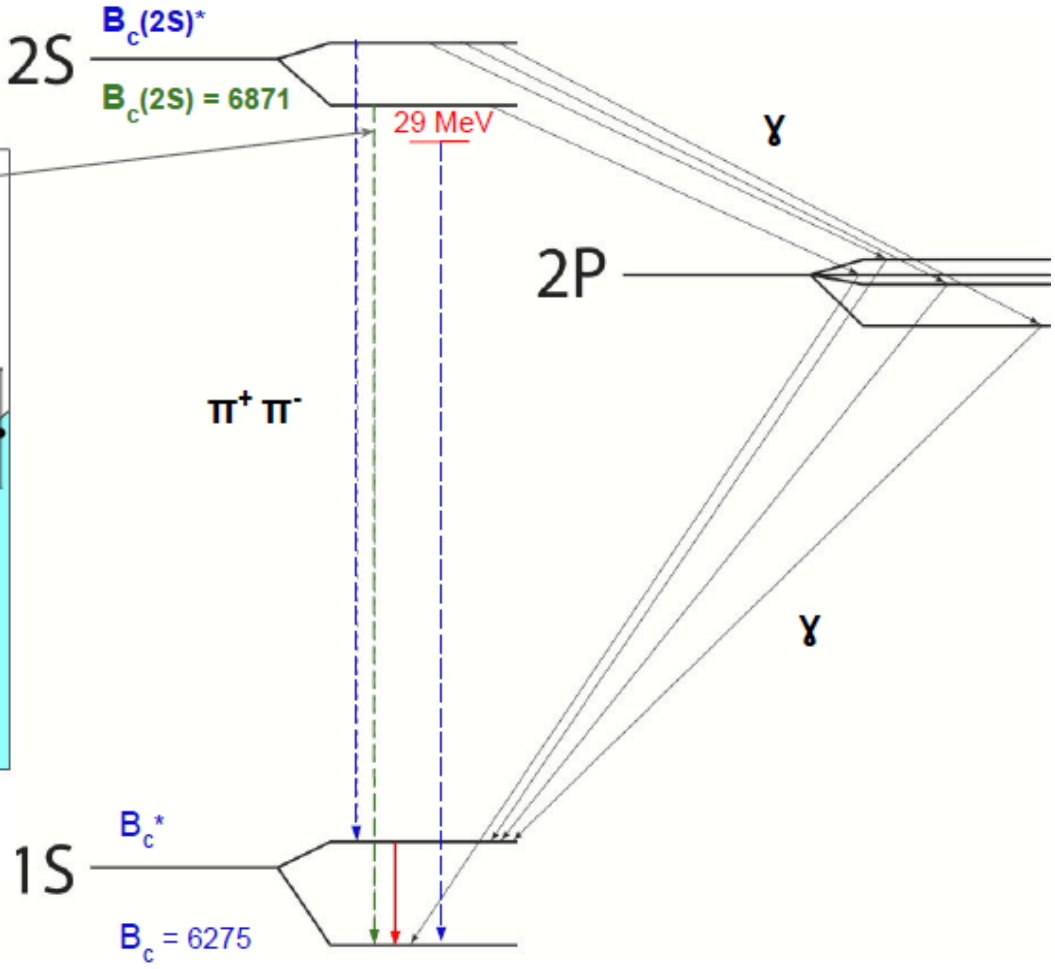

CMS-BPH-18-007

Summary (2)

Signals consistent with the $B_c(2S)$ and $B_c(2S)^*$ states have been separately observed for the first time by investigating the $B_c \pi^+ \pi^-$ invariant mass spectrum measured by CMS

The analysis is first LHC result based on the full usable Run 2 data of proton-proton collisions at a center-of-mass energy of 13 TeV, corresponding to a total integrated luminosity of 140 fb^{-1}

The two-peaks are very well resolved with a measured mass difference of **$\Delta M = 29.0 \pm 1.5$ (stat) $\pm$ 0.7 (syst) MeV**

Both peaks have local significance exceeding five standard deviations

The mass of the $B_c(2S)$ state is measured to be **$M(B_c(2S)) = 6871.0 \pm 1.2$ (stat) $\pm$ 0.8 (syst) $\pm$ 0.8 (B_c) MeV**

The mass of the $B_c(2S)^*$ state remains unknown because the B_c^* decays to $B_c \gamma$ and the photon is not reconstructed

Additionally two mass differences unaffected by the uncertainty of B_c world-average-mass, have been determined

$M(B_c(2S) - M(B_c) - 2m_\pi = 317.0 \pm 1.2$ (stat) $\pm$ 0.8 (syst) MeV and **$M(B_c(2S)^* - M(B_c^*) = 567.1 \pm 1.0$ (stat) MeV**

These measurements contribute significantly to the detailed characterization of the B_c family and provide a rich source of information on the non-perturbative QCD processes that bind heavy quarks into hadrons.

Fast response of LHCb:

Observation of an excited B_c^+ state

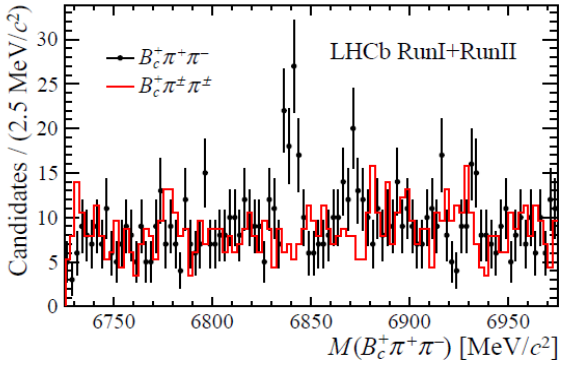

Figure 2: Invariant mass $M(B_c^+\pi^+\pi^-)$ distributions for the (black) data and (red) same-sign samples. The mass $M(B_c^+\pi^+\pi^-)$ is calculated with constraints on the J/ψ mass, B_c^+ mass and PV. The same-sign sample is normalised to the scale of the right-sign data sample as described in the text.

LHCb collaboration[†]

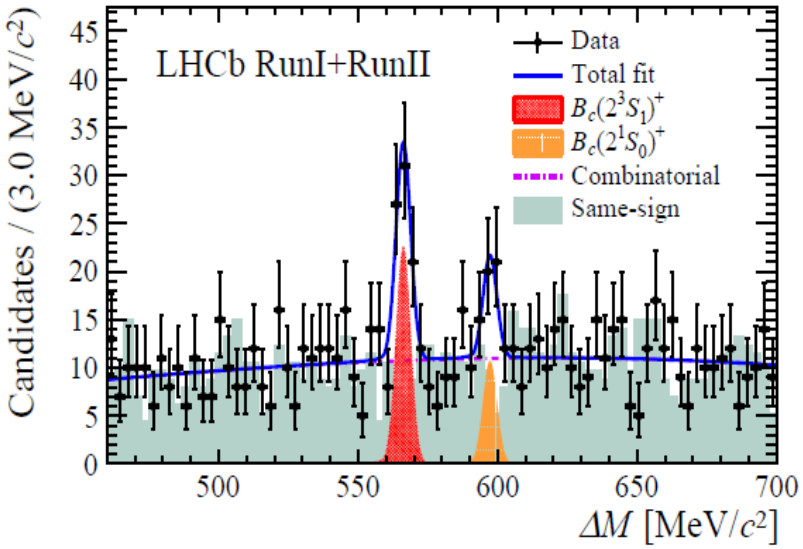

Figure 3: Distribution of ΔM with the fit results overlaid. Black points with error bars represent the data. The blue solid line is the fit to data. The red cross-hatched area show the $B_c(2^3S_1)^+$ signal component. The orange hatched area is the $B_c(2^1S_0)^+$ signal component. The violet dashed line is the combinatorial background. The dark green shaded area represents the ΔM distribution of the same-sign sample, which is normalised to the right-sign data sample as described in the text.

А.Лиходед ОТФ

Why the ratio of twoPeaks are different?

Answers:
1. Pt interval for CMS is > 15 GeV;
2.Pt interval for LHCb is < 15 GeV.

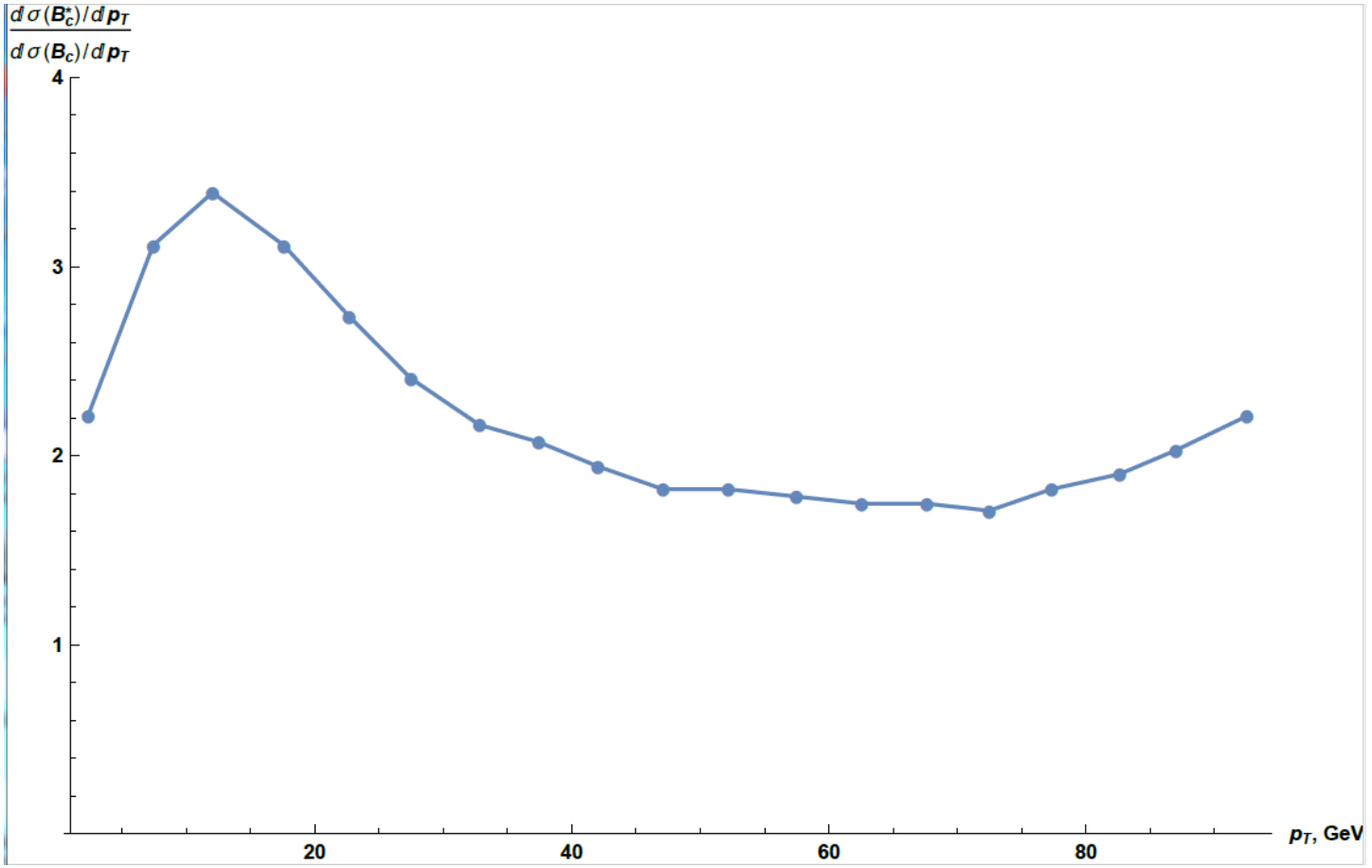

Thank you for your attention.